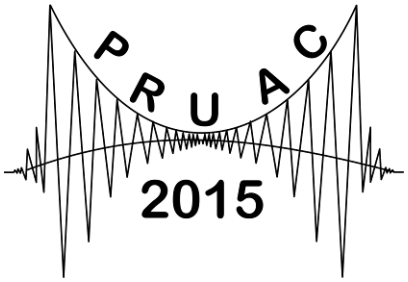

The 5th Pacific Rim Underwater Acoustics Conference

Vladivostok, Russia, 2015

PRUAC 2015
CONFERENCE PROGRAM

24 September 2015 (Thursday)

Time	**Session 3A. Acoustic tomography, geoacoustic inversion and ambient noise** **Chairs: Stanley Dosso and Jean-Pierre Hermand**	**Session 8. Other related topics** **Chairs: Fenghua Li and Luybov' Statsenko**
09.00 -- 09.20	A.S. Shurup, **Sergey N. Sergeev**, V.V. Goncharov, A.I. Vedenev, O.A. Godin, N.A. Zabotin, M.G. Brown (Moscow State Univ., **Russia)** Retrieval of deterministic normal modes from cross-correlations of acoustic noise in shallow water	**Zafar Iqbal**, H.N. Lee (Gwangju Inst. of Sci. and Tech., **Korea)** Underwater acoustic channel model and variations due to changes in node and buoy positions
09.20 -- 09.40	**Dmitriy S. Strobykin,** A.V. Burenin**,** E.A. Voitenko**,** M.S. Lebedev (Il'ichev Pacific Oceanologica Inst., **Russia**) Study of possibilities of flow field acoustic monitoring by the reciprocal sounding method in conditions of very shallow water	**Gi Hoon Byun,** J.S. Kim **(**Korea Maritime and Ocean Univ., **Korea**) Improvement of an adaptive time-reversal mirror
09.40 -- 10.00	**S.H. Kim,** B.N. Kim, B.K. Choi, J.W. Kim (Korean Inst. of Ocean Sci. and Tech., **Korea)** Long range acoustic tomography modeling for water temperature estimation in the East Sea	Yu. Agrafonov, M. Agrafonov, I. Petrushin, **Bair B. Damdinov**, Sh. Tsydypov (Buryat State Univ., **Russia)** Radial distribution function for liquid near the solid surface
10.00 -- 10.20	**J.W. Kim,** B.K. Choi, D.W. Lee, M.S. Sim (Korean Inst. of Ocean Sci. and Tech., **Korea)** Acoustic detection method of cylindrical target using broadband sonar signal in water	
10.20 -- 10.40	**D.G. Han,** J.Yu. Na**,** J.W. Choi (Hanyang univ., **Korea)** Temporal and spatial variations of high ambient noise environment in Southern coast of Korea	
10.40 -- 11.00	V.V. Goncharov, A.S. Shurup, A.I. Vedenev, **Sergey N. Sergeev**, O.A. Godin, N.A. Zabotin, M.G. Brown, A.V. Shatravin (Moscow State Univ., **Russia)** Tomographic inversion of measured cross-correlations of ambient noise in shallow water using the ray theory	
11.00 -- 11.20	**Nikolai G. Bibikov,** O.N. Grubnik, S.V. Kosterin (Andreev Acoustical Inst., **Russia)** The statistical characteristics of the distribution of snapping shrimps clicks in the coastal waters of the Pacific shelf of Russia	

Proceedings of Meetings on Acoustics

Volume 24 http://acousticalsociety.org/

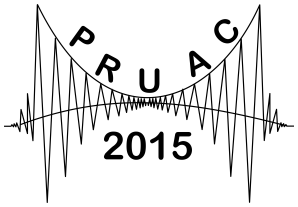

5th Pacific Rim Underwater Acoustics Conference

Vladivostok, Russia
23-26 September 2015

Underwater acoustic channel model and variations due to changes in node and buoy positions

Zafar Iqbal and Heung-No Lee
School of Information and Communications, Gwangju Institute of Science and Technology, Gwangju, Republic of Korea, 61005; zafar@gist.ac.kr; heungno@gist.ac.kr

The underwater acoustic channel (UAC) is known to offer poor communication channel and very limited transmission bandwidth. The channel is highly frequency selective and the channel response changes over time due to variations in channel conditions. Designing a system to deal with the frequency and time selective channel in UAC, therefore, becomes very challenging. Attempts were made to solve this problem by modeling the underwater acoustic channel, using a coded orthogonal frequency division multiplexing (OFDM) system. A detailed explanation of the channel model is provided, which was used for the performance evaluation of the proposed system. Consideration was given, not only to the channel variation due to the positional changes of the node and buoy, but also to the shadowing effects caused by the surrounding objects near the transmitters. A low-density parity check (LDPC) coded OFDM (COFDM) system was designed to deal with the negative effects of deep sub-band fading problems in OFDM systems. The design is simulated over a realistic (lognormal fading) channel, which shows a robust performance of our designed system in comparison with the un-coded communication system.

Published by the Acoustical Society of America

 [DOI: 10.1121/2.0000102]
Received 05 October 2015; Published 02 November 2015

1. INTRODUCTION

Underwater acoustic communication has widespread applications in monitoring of the underwater environment, military/oceanic surveillance, underwater navigation, observation of radiation leaks, and exploring the underwater resources. These applications require sophisticated underwater sensor networks, therefore, reliable and robust underwater communication systems are needed to be deployed [1], [2].

In the present underwater communication systems, the acoustic wave is the major carrier due to its low attenuation characteristic [3]. However, the slow propagation speed (1500 m/s in normal condition) of acoustic waves leads to long delay spread. Further, the underwater acoustic channel (UAC) is time varying according to changes in temperature, geometry of the channel, roughness of the sea surface, and spatial position determined by the sea current etc. In particular, multipath delay spread due to reflections at the sea surface and bottom causes inter-symbol interference (ISI) and frequency selective fading. Hence, these factors lead to system performance falloffs [4], [5].

To overcome such performance falloffs, the coded orthogonal frequency division multiplexing (COFDM) system has been proposed as one of the solutions, using the low density parity check (LDPC) codes [6], [7], turbo codes, and Reed-Solomon codes [8] in OFDM systems over UAC. However, most of these works use channel models that are overly simplified to test the system performance, e.g., (*i*) employing too few multipath components, (*ii*) overlooking channel variation according to the positional change in the configuration of the node and buoy, and (*iii*) shadowing effects caused by the surrounding objects.

The authors in [1], [9], and [10] describe challenges such as noise, Doppler spreading effects, multipath fading, and shadow zones, in the design of underwater acoustic sensor networks, along with a detailed characterization of UAC. It is still considered a significant research problem to design an underwater acoustic sensor network system that performs robustly over the UAC, which exhibits many challenges as mentioned above.

The purpose of this paper is to propose an underwater COFDM scheme for wireless underwater sensor networks and show its robust performance against the challenging UAC problems. The envisioned network is a wireless sensor access network where multiple sensors in shallow water transmit to a buoy on the sea surface. A detailed explanation of the channel and system model is provided, which was used for the performance evaluation of the proposed system. We consider, not only the channel variation due to the positional changes of the node and buoy but also the shadowing effects caused by the surrounding objects near the transmitters.

2. CHANNEL MODEL

Since there are many conditions affecting the underwater channel, it is difficult to consider all these conditions in modeling the channel [1]. Due to this reason, many researchers have modeled the UAC under the flat condition on the sea surface and bottom to reduce the complexity and make it easier to analyze [11]. However, these works do not clearly mention the modeling procedure for the UAC and only list the characteristics of the UAC. In this paper, we aim to describe the modeling procedure step by step, as well as channel characteristics.

A. DOPPLER SPREAD

The surface scattering of UAC depends on the sea surface condition. Under an ideally flat surface condition, incident waves are almost perfectly reflected with a phase shift of π. However, under practical conditions, swells lead to movement of the reflection point and create energy dispersion. The Doppler spread with a carrier frequency f kHz [12] is represented as follows,

$$f_D = (0.0175/c) f . w^{3/2} . \cos\theta \tag{1}$$

where c, w and θ are sound speed, sea surface wind speed, and grazing angle, respectively. Sound speed is affected by salinity, water temperature, pressure, etc., but it is 15 m/s under normal conditions. Fig. 1 shows the Doppler spread against the carrier frequency and sea surface wind speed when we assume $\cos\theta = 1$ in Eq. (1). This figure depicts a geometric Doppler spread increase using a higher carrier frequency. Although using a higher carrier frequency has an advantage (i.e., increase of available transmission bandwidth), it also has a disadvantage (i.e., geometric increase of the Doppler spread). Thus, this trade-off relationship should be considered for the communication system design over UAC.

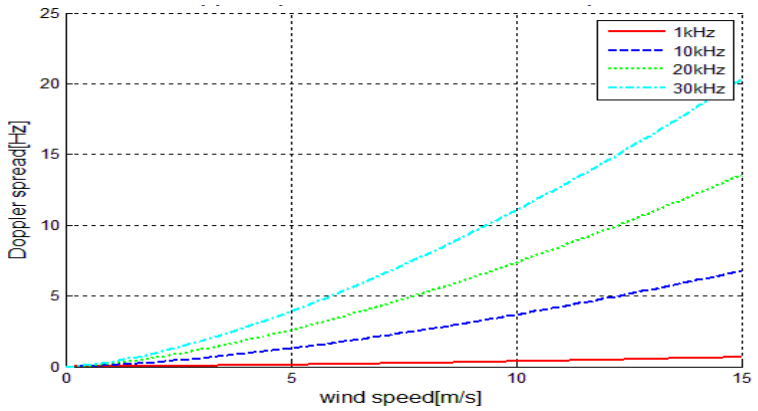

Fig. 1. Doppler spread caused by reflection on the sea surface

B. MULTIPATH

In UAC, the acoustic waves are reflected on the sea surface and bottom, and form the multipath as shown in Fig. 2(a) [5], [9]. The reflection paths are classified into four types based on the total number of reflections (odd or even) and the first reflection point (surface or bottom).

Fig. 2 (b) and (c) show such classification in terms of total number of reflections. Fig. 2(b) shows the multipath reflected odd number of times. The red rays (*i*) is a case where the first reflection occurred on the sea surface and the blue rays (*ii*) is a case where the first reflection occurred on the bottom. Similarly, Fig. 2(c) shows the multipath reflected even number of times. The violet rays (*iii*) and green rays (*iv*), show the first reflection occurred on the sea surface and bottom, respectively. These rays can be limited in the special cases. In case the buoy is located on the ocean bottom, the generation of blue rays (*ii*) and green rays (*iv*) is limited. Similarly, red rays (*i*) and green rays (*iv*) cannot be created when the buoy is located on the sea surface. In case the node and buoy are located on the sea bottom and surface, individually, there is only one set of creatable rays, i.e., violet rays (*iii*).

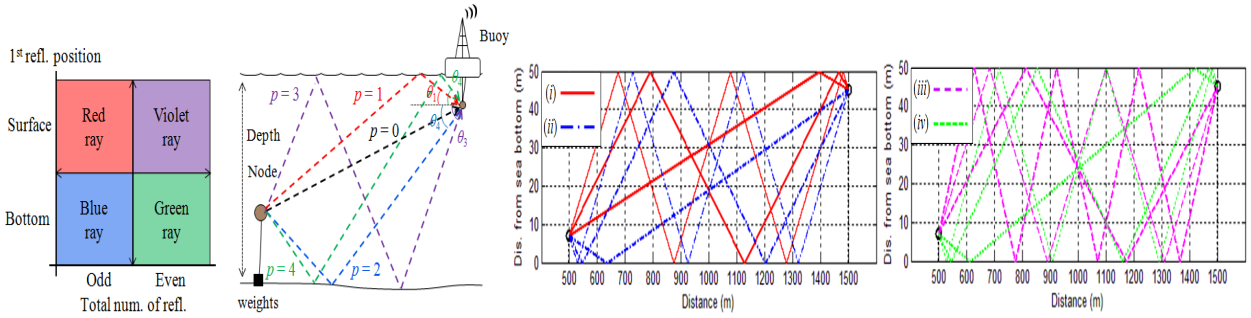

(a) *(b)* *(c)*

Fig. 2. Classification of multipath: (a) multipath over UAC; (b) multipath reflected odd number of times; (c) multipath reflected even number of times.

C. FREQUENCY RESPONSE

The frequency response of each reflection path is represented as a function of frequency, number of reflections, and distance of the path. The frequency response of the p-th path is,

$$\overline{H}_p(f) = \frac{\Gamma_p}{\sqrt{A(l_p, f)}} \tag{2}$$

where $A(l_p, f)$ is the single path attenuation with distance l_p m and carrier frequency f Hz. In addition, Γ_p is the reflection coefficient, which is calculated by using the number of times a ray reflected from the sea surface (n_{sp}) and bottom (n_{bp}) [13]. The calculations of such factors are as follows.

The reflection coefficient Γ_p is,

$$\Gamma_p = \gamma_s^{n_{sp}} \gamma_b^{n_{bp}}(\theta_p) \tag{3}$$

where γ_s and γ_b are the reflection coefficients at the sea surface and bottom, respectively. In addition, θ_p is the grazing angle. Under flat sea surface condition, γ_s is approximated as -1 and γ_b is calculated as follows.

$$\gamma_b(\theta) = \begin{cases} \dfrac{\rho_b \sin\theta - \rho\sqrt{(c/c_b)^2 - \cos^2\theta}}{\rho_b \sin\theta + \rho\sqrt{(c/c_b)^2 - \cos^2\theta}} & , \cos\theta \le c/c_b \\ 1 & otherwise \end{cases} \tag{4}$$

where ρ and c are the sea surface layer water density and sound speed; and, ρ_b and c_b are the density and sound speed at the sea bottom. We chose the values for these parameters as 1022 kg/m^3, 1526 m/s, 1027 kg/m^3, and 1490 m/s, respectively [14], [15].

In (2), the single path loss $A(l_p, f)$ is,

$$A(l_p, f) = A_0 \cdot l_p^{\,k} \cdot a(f)^{l_p} \tag{5}$$

where A_0 is a constant scaling factor and k is a spreading factor between 1 and 2, according to the type of spreading. In this paper, we set A_0 as 1 and k as 2, considering spherical spreading. $a(f)$ is

an absorption coefficient expressed as $a(f) = 10^{\alpha(f/1000)/10000}$. In (5), $\alpha(f)$ is defined by Thorp's empirical formula [10] as,

$$\alpha(f) = 0.11\frac{f^2}{1+f^2} + 40\frac{f^2}{4100+f^2} + 2.75\times10^{-4}\cdot f^2 + 0.003\ . \tag{6}$$

It is necessary to calculate the distance of reflection path since the single path loss aforementioned is composed of a function of carrier frequency and distance of the path. Similarly, the grazing angle is an essential factor to calculate the reflection coefficient.

To calculate the distance, we used the Pythagorean Theorem. We start with an example to illustrate the proposed method, as shown in Fig. 3. To calculate the distance of reflection path from *A* to *B*, i.e., dashed line, (*i*) move *B* to *B'* against the sea surface, (*ii*) calculate the length of the base line, i.e., *d*, (*iii*) calculate the height of the triangle, i.e., $2h - a - b$ since the distance from surfact to point *A'* is $h - a$ and from sea surface to *B'* is $h - b$, and (*iv*) calculate the distance by using the Pythagorean Theorm, which is $l_p^2 = d^2 + (2h - a - b)^2$.

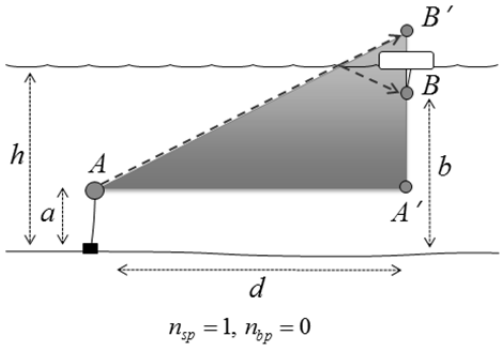

Fig. 3. Example of reflection path

We aimed at applying such an approach to more complex cases and obtained general equations for the distance of reflection path as,

$$l_p = \sqrt{d^2 + (2h\cdot n_{sp} + \alpha a + \beta b)^2} \tag{7}$$

where α and β are classification values according to the first reflection point (surface or bottom) and the total number of reflections (odd or even). In particular, $(\alpha, \beta) = (-1, -1)$ is a classification value for the reflection path having first reflection on the surface and total odd number of reflections, i.e., red rays (*i*) in Fig. 2. Other cases, i.e., $(\alpha, \beta) = (+1, +1)$, $(-1, +1)$, and $(+1, -1)$ are for reflection paths like blue rays (*ii*), i.e., having first reflection on the bottom and odd number of reflections, violet rays (*iii*), i.e., having first reflection on the surface and even number of reflections, and green rays (*iv*), i.e., having first reflection on the bottom and even number of reflections.

Using the parameters d, h, n_{sp}, a, b, α, and β (distance, depth, number of reflections on sea surface, distance from the bottom to the node and to buoy, and classification factors) in these equations, the distances of all possible reflection paths can be calculated easily.

After calculating the distance of all possible reflection paths, the grazing angle can also be calculated, as $\theta_p=\cos^{-1}(d / l_p)$.

D. IMPULSE RESPONSE

The impulse response of UAC while considering such reflection characteristics can be modeled as,

$$h(t) = \sum_p h_p(t - \tau_p) \tag{8}$$

where h_p is an inverse Fourier Transform of the p-th path frequency response and $\tau_p = (l_p - l_0)/c$ is the arrival time difference between the direct path and each p-th path.

3. SYSTEM MODEL

Since Doppler spread increases geometrically, as the carrier frequency increases [12], to overcome time selective fading, we should select a carrier frequency that is as low as possible. However, the use of a very low carrier frequency causes a limitation of the available transmission bandwidth. In this paper, we chose a 7 kHz carrier frequency assuming the use of 10 kHz bandwidth. Such a bandwidth is based on the typical bandwidths of UAC for different ranges. Since we assume the distance is 1000 m, i.e., *medium* range, approximately 10 kHz bandwidth is suitable to our system [4]. In addition, to overcome the ISI problem, we set the cyclic prefix (CP) period as 25 ms via analysis of the impulse response of the modeled channel. Under this setting, the Doppler spread, maximum delay spread, and coherent time of the channel are about 4.744 Hz, 25 ms, and 210 ms, respectively [16].

It is essential to choose a number of sub-carriers that satisfy the conditions to overcome frequency selective fading ($\Delta f \leq B_c$) and time selective fading ($T_s << T_c$) to deal with both problems at the same time. In this paper, we chose 256 sub-carriers to satisfy these conditions. Consequently, the valid symbol duration and the CP period is 25.6 ms and 25 ms, respectively. The suggested OFDM system is able to overcome not only frequency selective fading, since the sub-carrier bandwidth (39.0625 Hz) is smaller than the coherent bandwidth of the channel (40 Hz); but also ISI, since CP period (25 ms) is larger than or equal to the maximum delay spread; as well as time selective fading, since the OFDM symbol duration (50.6 ms) is sufficiently smaller than the coherent time of the channel (210 ms).

In order to add the LDPC code to the OFDM system, we consider regular LDPC codes, which are represented as (n, j, k) where n is the block length and j and k are the number of ones on each row and column of the parity check matrix, respectively [17]. We set j and k to 4 and 8, respectively, and set the block size n to 256, which is same as the number of sub-carriers to combine with the previously designed OFDM system.

4. SIMULATION SETTINGS

Our simulation channel model assumes a water depth of 50 m and a maximum sea surface wind speed of 15 m/s, with a distance of 1000 m separating the node and buoy as shown in Fig.

4. We select the parameters with an aim to design realistic channel conditions. Especially, 50 m depth is approximated while considering the average depth of the Korean Western Sea, i.e., 44 m. We set the node and buoy at 7 m and 45 m height from the sea bottom, respectively. In addition, we assume the node and buoy can be located at various depths to observe performance variations according to the channel conditions. So, a node can be located at one of {0, 1, 3, 5, 9, 11, 13, 15, 17} m, as well as 7 m. In the case of buoy, a possible location is one of {20, 25, 30, 34, 40, 41, 43, 47, 49, 50} m, as well as 45 m.

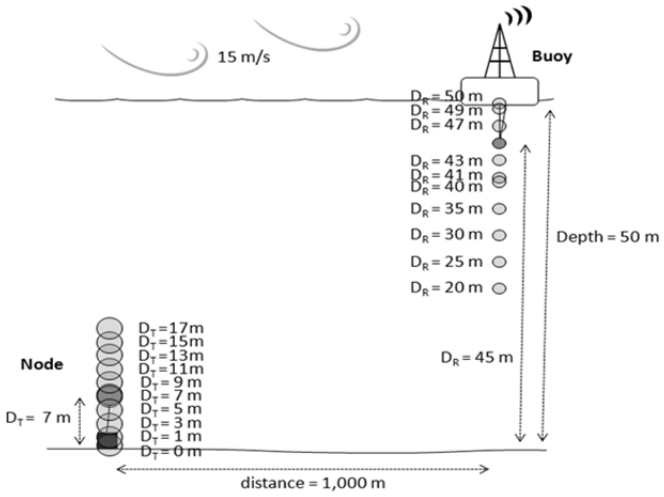

Fig. 4. Simulation channel setting

Fig. 5 (a)-(d) shows the impulse responses of some parts of the simulation channels described above. Analyzing these results, the maximum delay spread and coherence bandwidth are found to be about 25 ms and 40 Hz, respectively. In addition, Fig. 5(b)-(d) shows the limited multipath creation according to the position of the node and buoy. In Fig. 5(b), the multipath occurring with the first reflection on the bottom (p=2 and p=4 in Fig. 2) is limited since the node is located on the bottom. Similarly, in Fig. 5(c), the multipath having a last reflection on the surface (p=1 and p=4 in Fig. 2) cannot be created since the buoy is located on the sea surface. For the same reasons, looking at the channel in Fig. 5(d), creation of multipath occurring with the first reflection on the bottom and the last reflection on the surface is limited. Consequently, the special cases, when the node and buoy are located on the sea surface and/or bottom, even though the change in the node and buoy depth is small, result in wide performance variation.

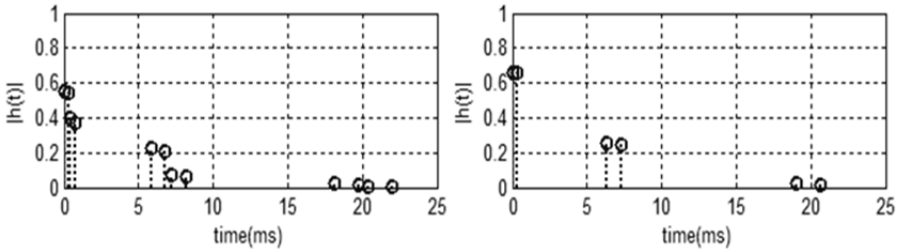

(a) D_T = 7 m, D_R = 45 m *(b) D_T = 0 m, D_R = 45 m*

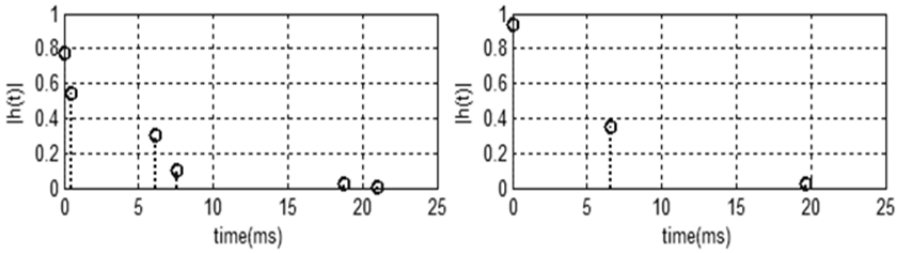

(c) D_T = 7 m, D_R = 50 m *(d) D_T = 0 m, D_R = 50 m*

Fig. 5. The normalized impulse response of the UAC model

5. PERFORMANCE ANALYSIS

In this section, we analyze the bit-error rate (BER) performance of the suggested LDPC coded OFDM system. The results show the overcoming of the performance falloff via the LDPC code. In detail, over a certain threshold of the received SNR, the designed system is able to solve the performance falloff problem caused by deep fading at certain specific sub-carriers. To be specific, this system not only achieves a 17 dB SNR benefit, but also reduces the SNR variation, due to channel conditions. This reduction of the SNR variations is shown in the Fig. 6 and Fig. 7. Using LDPC coded OFDM system, the SNR variation reduced noticeably from ~10 dB to ~3 dB at the 10^{-3} BER point versus the un-coded OFDM system. These results mean that we can assure robust performance even if the positions of the node and buoy are changed in the underwater environment.

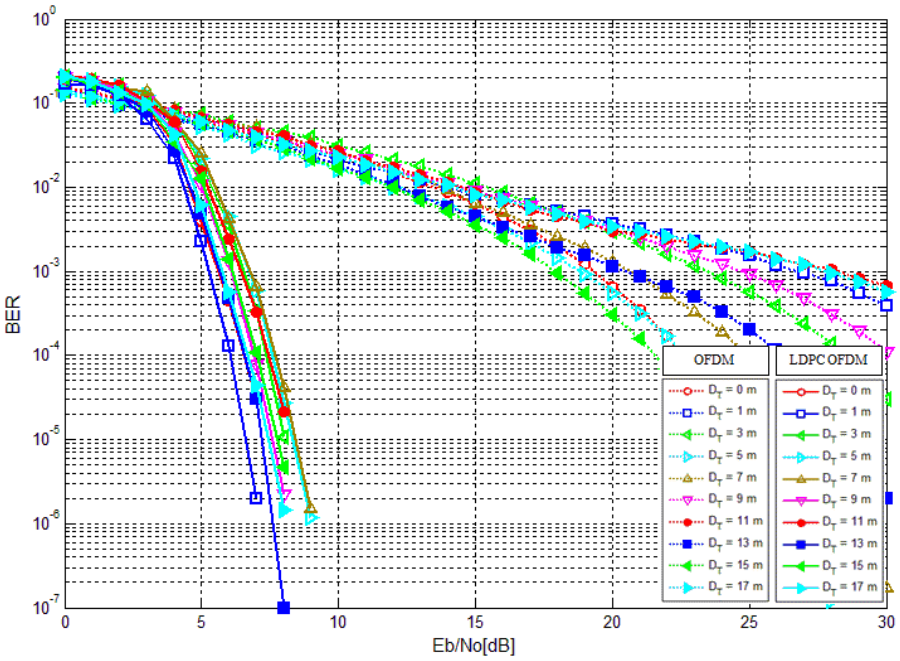

Fig. 6. Performance of LDPC coded ODFM system (D_T variation, D_R = 45 m)

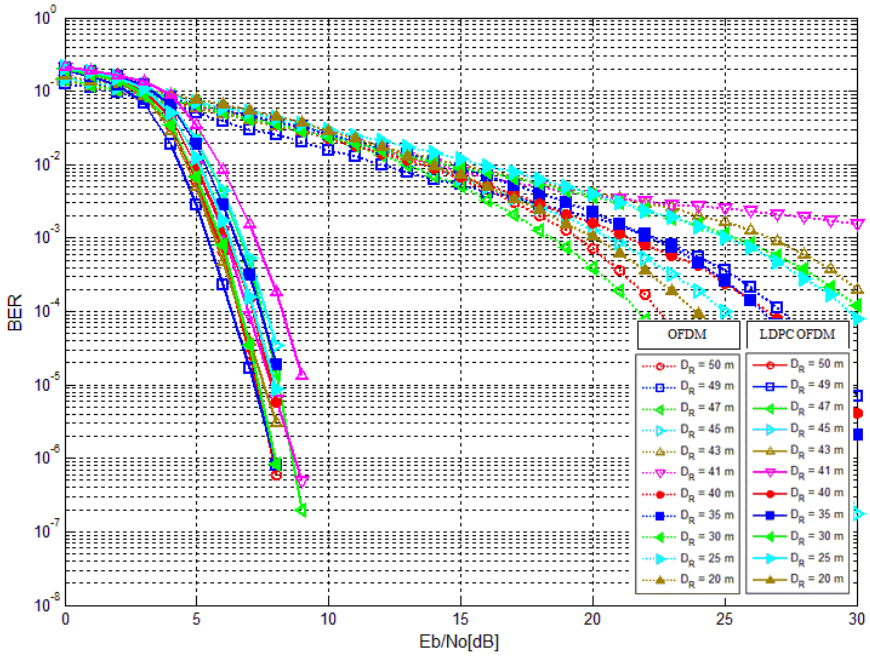

Fig. 7. Performance of LDPC coded ODFM system (D_T= 7 m, D_R variation)

A. LOGNORMAL FADING FOR UNDERWATER CHANNEL

Until now, we have suggested the LDPC coded OFDM system as one of the solution to obtain robust performance in UAC. However, there are some problems to apply it to realistic systems. We have assumed almost flat condition of the sea surface and bottom so far but this assumption does not fit perfectly to realistic systems. Although the channel seems to be ideally

flat in the broader sense, there are some rocks, coral reefs, pebbles, cracks, slopes, etc. that causes fading effects. Thus, we modeled such fading effects as a lognormal random distribution [18], [19].

Fig. 8 compares the performance of the uncoded OFDM system and LDPC coded OFDM system, according to lognormal fading. Although we used the LDPC code to mitigate negative deep fading effect at certain specific sub-carriers, we need ~18 dB SNR to obtain 10^{-3} BER performance, which shows a robust performance as compared to the uncoded system but emphasizes that the realistic channel still needs a higher SNR to achieve the same performance.

These fading effects can be overcome via user cooperation based on LDGM codes, which is left as a future work.

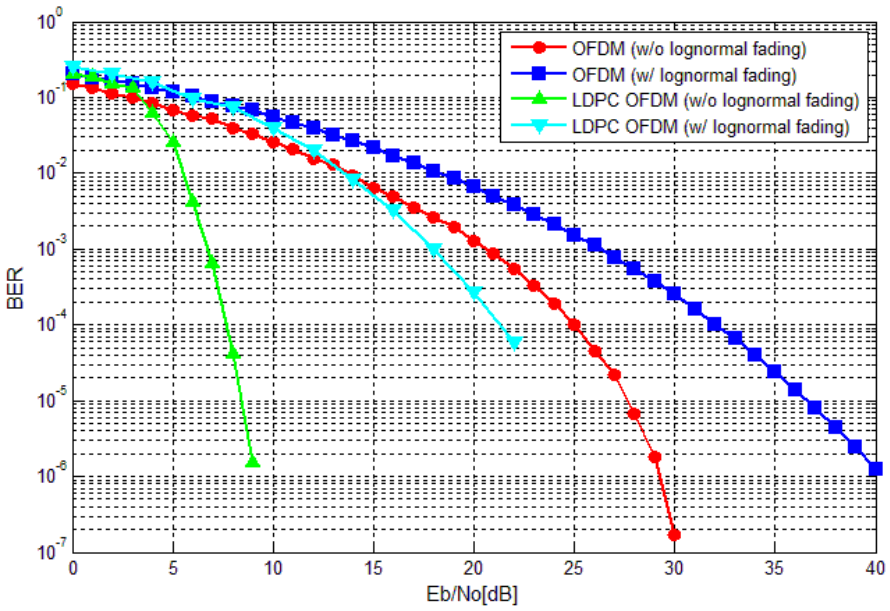

Fig. 8. Performance of the LPDC coded OFDM system under lognormal fading

6. CONCLUSION

In this paper, we characterized the underwater acoustic channel and provided a channel model for performance evaluation via computer simulations. A simulation channel model is used for evaluation of the proposed coded OFDM system in the UAC. It is obtained under the assumption of very poor communication conditions such as 15 m/s maximum wind speed on the sea surface causing time-selective channel impulse response, and a number of reflected multipath causing frequency selective channels. To set up a robust communication system over the test channel, we set the OFDM system parameters carefully to overcome the problems of multipath induced inter symbol interference, frequency-selective, and time-selective fading.

Simulation results show the robustness of the proposed system by reducing the required SNR to achieve a specific BER. The variation in performance due to changes in node and buoy positions has also been reduced to ~3 dB from ~10 dB. Finally, the design is applied to a realistic underwater acoustic channel to observe its performance and a future plan has been given.

ACKNOWLEDGMENTS

This work was supported by the National Research Foundation of Korea (NRF) grant funded by the Korean government (NRF-2015R1A2A1A05001826).

This research was supported by Leading Foreign Research Institute Recruitment Program through the National Research Foundation of Korea (NRF) funded by the Ministry of Science, ICT and Future Planning (MSIP) (2009-00422). And this research was a part of the project titled 'Development of Ocean Acoustic Echo Sounders and Hydro-Physical Properties Monitoring Systems', funded by the ministry of Ocean and Fisheries, Korea.

REFERENCES

[1] I. F. Akyildiz, D. Pompili, and T. Melodia, "Underwater acoustic sensor networks: research challenges," *Elsevier Ad Hoc Networks,* vol. 3, pp. 257-279, Mar. 2005.

[2] D. B. Kilfoyle and A. B. Baggeroer, "The state of the art in underwater acoustic telemetry," *IEEE Jr. Oceanic Engineering*, vol. 25, no. 1, pp. 4-27, Jan. 2000.

[3] L. Liu, S. Zhou, and J.-H. Cui, "Prospects and problems of wireless communication for underwater sensor networks," *Wiley Wirel. Commun. Mob. Comput. Sp. Issue on Underwater Sensor Networks*, vol. 8, no. 8, pp. 977–994, Oct. 2008.

[4] I. F. Akyildiz, D. Pompili, and T. Melodia, "Challenges for efficient communication in underwater acoustic sensor networks," *ACM SIGBED Rev.*, vol. 1, no. 2, pp. 3-8, Jul. 2004.

[5] M. Stojanovic and J. Preisig, "Underwater acoustic communication channels: Propagation models and statistical characterization," *IEEE Communications Magazine*, vol. 47, no. 1, pp. 84-89, Jan. 2009.

[6] L. Bai, F. Xu, R. Xu, and S. Zheng, "LDPC Application Based on CI/OFDM Underwater Acoustic Communication System," *1st Int. Conf. Information Science and Engineering (ICISE)*, pp. 2641-2644, 26-28 Dec. 2009.

[7] J. Huang, S. Zhou, and P. Willett, "Nonbinary LDPC coding for multicarrier underwater acoustic communication," *IEEE JSAC Special Issue on Underwater Wireless Communications and Networks*, vol. 26, no. 9, pp. 1684–1696, Dec. 2008.

[8] L. Litwin and M. Pugel, (2001, Jan.) "The Principles of OFDM," *RF Signal Processing*, pp. 30-48. [Online] Available: http://www.rfdesign.com

[9] M. C. Domingo, "Overview of channel models for underwater wireless communication networks," *Elsevier Physical Communication*, vol. 1, no. 3, pp. 163-182, Sep. 2008.

[10] L. M. Brekhovskikh and Y. P. Lysanov, *Fundamentals of Ocean Acoustics,* 3rd Ed. New York: Springer-Verlag, 2003.

[11] A. G. Zajic, "Statistical modeling of MIMO mobile-to-mobile underwater channels," *IEEE Trans. Vehicular Technology*, vol.60, no.4, pp.1337-1351, May 2011.

[12] M. Stojanovic, 1999. "Underwater Acoustic Communication," *Wiley Encyclopedia of Electrical and Electronics Engineering*, John Wiley & Sons, 1999, vol.22, pp.688-698.

[13] M. Stojanovic, "Underwater acoustic communications: design considerations on the physical layer," *Fifth Ann. Conf. Wireless on Demand Network Systems and Services, (WONS) 2008,* pp.1-10, Jan. 2008.

[14] K. V. Mackenzie, "Nine-term equation for sound speed in the oceans," *Jr. Acoustical Soc. America*, vol. 70, no. 3, pp. 807-812, Sep. 1981.

[15] F. J. Millero, C. T. Chen, A. Bradshaw, and K. Schleicher, "A new high pressure equation of state for seawater," *Elsevier Deep Sea Research Part A*, vol. 27, no. 3-4, pp. 255-264, Apr. 1980.

[16] B. Sklar, Digital Communications: Fundamentals and Applications, 2nd Ed., Prentice Hall, 2001.

[17] R. G. Gallager, *Low-Density Parity-Check Codes,* M.I.T. Press, 1963.

[18] M. Evans, N. Hastings, and B. Peacock, *Statistical Distributions,* Hoboken, NJ: Wiley-Interscience, 2000.

[19] W.-B. Yang and T. C. Yang, "High-frequency channel characterization for M-ary frequency-shift-keying underwater acoustic communications," *Jr. Acoustical Soc. America,* vol. 120, no. 5, pp. 2615-2626, Nov. 2006.